ChemistrySelect

Research Article
doi.org/10.1002/slct.202505203

Chemistry Europe
European Chemical Societies Publishing

www.chemistryselect.org

Magnetic Behavior Affected by Structural Properties in Sputtered Co/Cu Multilayers: Effect of Total Thickness and Deposition Rate

Leman Gökçen Gerelegiz,[a] Ali Karpuz,*[a] Nadir Kaplan,[b] and Hakan Köçkar[b]

Co/Cu multilayer films were produced by the sputtering technique in two series: by changing the total thickness, and by considering different deposition rates of the Co layer. The surface roughness increased with an increase in the total film thickness, and the increase in the coercivity (H_c) value was associated with this increase in surface roughness. As the deposition rate of the Co layer increased, the intensity of the peak belonging to the (111) plane of the face-centered cubic structure of Cu and the crystallite sizes decreased. With an increase in the deposition rate, the Co atomic content gradually increased, the M_s value increased accordingly, and the H_c value decreased. In addition, the film surfaces became smoother, and a slight decrease in the size of the grains on the surface was observed with an increase in the deposition rate of the Co layer. The structural and magnetic properties of the Co/Cu films were affected by the different total thicknesses of the films and the change in the deposition rate of the Co layer. This study contributes to the lack of studies on the magneto-structural properties of DC sputtered Co/Cu multilayers. This allows the magnetic properties to be tuned for specific applications using Co/Cu films.

1. Introduction

The need for nanomagnetic materials is constantly increasing in technologies where magnetic nanomaterials are used because of their wide range of applications.[1,2] Studies have shown that nanomagnetic materials are quite successful and efficient in read-write heads, magnetic recording devices and magnetic sensor applications and they have played a key role in these technologies.[3–6] The structure of sputtered Co/Cu multilayers was investigated in a previous study,[7] and it was noted that these multilayers are quite suitable for use in sensor devices. Similarly, in another study done by Tekgül et al.,[8] it was emphasized that Co/Cu multilayer thin films are important for magnetic sensor applications. The DC magnetron sputtering technique is a prominent technique for thin film production because of the strong adhesion of the films to the substrate surface and the controllability of the production parameters.[9,10] The physical properties of multilayer films produced by sputtering technique are closely dependent on the production conditions and parameters. The structural and magnetic properties of thin films produced by changing the characteristic parameters, such as layer thickness, substrate type, temperature, total thickness, and deposition rates of the layers have been investigated in many studies.[11−13] In previous years, many studies have been conducted on the synthesis and characterization of Co/Cu multilayer films using the electrodeposition technique.[14,15] Besides, many studies have been conducted on the properties of sputtered Co/Cu multilayers. Kondratev et al. investigated the atomic separation achieved by hybrid X-ray reflectivity in Co/Cu/Co multilayer.[16] A recent study by Tokaç [17] performed a comparative analysis of the magnetic properties as a function of the Co thickness in Co/Cu multilayers produced using DC magnetron sputtering. Zhang et al.[18] investigated the magnetic properties of $[Co/Cu]_2$ by changing the roughness variation due to the thickness of the nonmagnetic layer film. In addition, Dalouji et al.[19] recently reported a detailed study on the surface topography of Cu/Co bilayers. According to our findings, there is a clear deficiency in the investigation of the subject of this study, especially regarding the effect of the Co deposition rate in Co/Cu multilayer films produced by the DC magnetron sputtering technique. Therefore, it is anticipated that reporting the microstructure and magnetism correlation of Co/Cu films will provide a new perspective in this field and an enlightening support for subsequent studies. In this study, Co/Cu multilayer films were produced using the DC magnetron sputtering method, and two separate series were produced to investigate the dependence of the properties of Co/Cu films on different total film thicknesses and Co deposition rates. Structural and magnetic analyses of the films were performed and their suitability for applications in magnetic film technology was investigated.

2. Experimental Section

The Co/Cu films examined in this study were produced on polymeric acetate substrates in two separate series using the DC magnetron sputtering technique. Detailed information on the production of

---

[a] *L. G. Gerelegiz, A. Karpuz*
Department of Physics, Kamil Özdağ Science Faculty, Karamanoğlu Mehmetbey University, Karaman, Türkiye
E-mail: alikarpuz@kmu.edu.tr

[b] *N. Kaplan, H. Köçkar*
Department of Physics, Science and Literature Faculty, Balıkesir University, Balıkesir, Türkiye

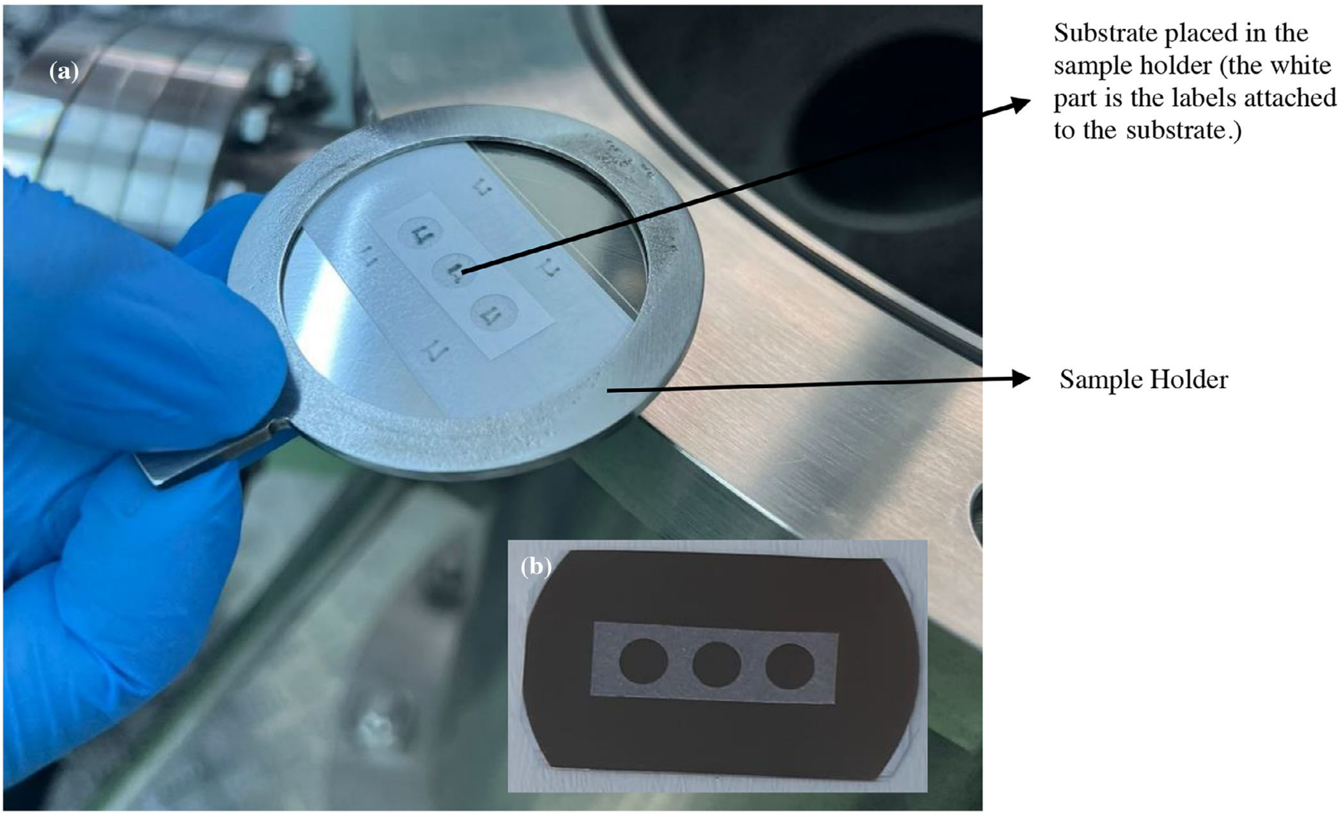

Figure 1. a) A substrate placed in the sample holder (before production). b) The acetate substrate and thin film produced on the substrate (inset).

many types of thin films using the sputtering technique can be found in.[20] In the first series, the number of bilayers was changed to 6, 7, and 8, and the total thickness of the magnetic thin films was determined to be 120, 140, and 160 nm. While producing this series of films, the deposition rate of Co and Cu layers was kept constant at 0.04 nm/s, and the thickness values of Co and Cu layers were 8 and 12 nm, respectively. These films were formulated as A[Cu(12 nm)/Co(8 nm)], A = 6, 7, 8 (A = bilayer Number) for 120 nm, 140 nm, and 160 nm, respectively. In the second series, the number of bilayers was kept constant at 5, the thickness of the Co layer at 10 nm, and the thickness of the Cu layer at 8 nm, with a total thickness of 90 nm. Considering these values, the films were represented by the expression 5[Cu(8 nm)/Co(10 nm)]. The Cu deposition rate was 0.04 nm/s, while the deposition rate of the Co layer was changed to 0.02, 0.05, and 0.08 nm/s, separately. For the production of films, 2.0 mm thick Cu and 1.2 mm thick Co targets with 99.99% purity were used. The diameter of the targets placed in the magnetrons was 50.8 mm. Before starting the film production, the inside of the vacuum chamber, magnetrons, and sample holder located on the cover of the vacuum chamber were cleaned with isopropyl alcohol. The nonmagnetic, 0.12 mm thick, commercial and flexible polymeric acetate substrates on which the films were grown were cut to the desired dimensions (Figure 1) and then kept in isopropyl alcohol in the ISOLAB ultrasonic bath[21] for 10 min for sterilization.

When the pressure of the vacuum chamber dropped to $3x10^{-6}$ mbar, the suitable pressure value for production was reached, and the chamber was ready for the sputtering process. By introducing argon gas into the vacuum chamber, the pressure of the chamber increased to $4.5x10^{-3}$ mbar before the film deposition. The trend of the chamber pressure values was similar to that in.[22,23] First, argon gas, which was given at relatively high values for the easy formation of plasma, was reduced in a controlled manner to the ideal value for production (30 sccm, standard cubic centimeters per minute) after the plasma was formed. To start production, the shutter in front of the substrate was opened, and the thickness sensor (QCM, Quartz Crystal Microbalance) was activated simultaneously. The production was completed when the desired thickness was deposited. All thickness values were controlled using a QCM thickness monitor, as done in a recent study.[24] After production, the deposited films were preserved in a desiccator under a dry atmosphere and at a constant room temperature until film characterization.

Crystal structure analysis was performed using X-ray diffraction technique (XRD, BRUKER, D8 Advance with Davinci Design for XRD). The X-ray radiation was CuK_{α} ($\lambda = 0.15406$ nm). The Bragg angle (2θ) was varied between 30° and 80° with 0.2° step intervals to obtain the diffraction patterns of the samples. Elemental analysis was performed using energy dispersive X-ray spectroscopy (EDX) during the investigation of the surface morphology executed using a scanning electron microscope (SEM, HITACHI SU5000). Because the substrate used was electrically insulating, the electrical conduction required for SEM analysis was achieved by contacting the sample with conductive tape rather than applying a conductive coating on the sample. An atomic force microscope (AFM, NANOMAGNETIC INS. INC., hpAFM, Türkiye) with Image Analyzer V4.7 software was also used for roughness analysis of the surfaces of the film and substrate. The AFM characterization was performed by scanning a surface area of 8 x 8 μm^2. Magnetic properties of the multilayers were revealed using a vibrating sample magnetometer VSM (ADE TECHNOLOGIES, DMS-EV9) by cutting the sample into a circular form. The VSM system has a high resolution of $1x10^{-6}$ emu compared to the measured M_s of around 1×10^{-3} emu for the samples, thus negligible deflection of the results was observed. All measurements and analyses were accomplished at room temperature.

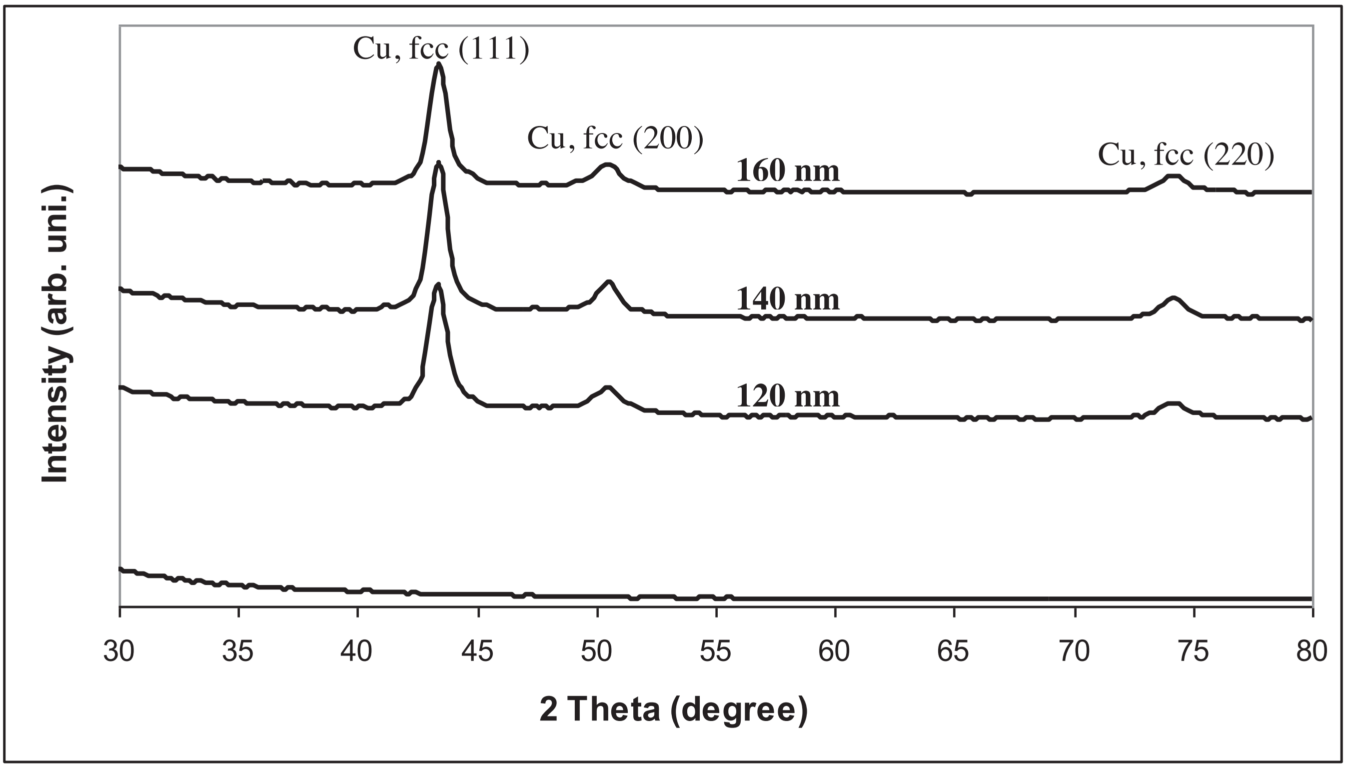

Figure 2. XRD patterns of the substrate and the Co/Cu multilayers with different total thicknesses.

3 Results and Discussion

3.1 Effect of Total Film Thickness

The atomic content of the film, with a thickness of 120 nm, consisted of 11% Co and 89% Cu atoms. On the other hand, the atomic contents of the films with total thicknesses of 140 nm and 160 nm consist of 12% and 15% Co and 88% and 85% Cu atoms, respectively. Considering the results, when the total film thickness was increased from 120 to 160 nm, the Co content of the films was 13 ± 2%. No significant change was observed in the atomic content of the magnetic thin films as the total thickness increased.

Diffraction patterns were examined to investigate the crystal structure. Before the deposition process, the crystal structure of the substrate was also determined. The diffraction patterns of the substrate and films are presented in Figure 2. No peaks corresponding to the substrate were observed in the diffraction pattern of the substrate. In the film with a thickness of 120 nm, a main peak is observed at $2\theta = 43.4°$, and other relatively smaller peaks are observed at $2\theta = 50.6°$ and $2\theta = 74.4°$. In the films with thicknesses of 140 and 160 nm, the same peaks were observed at almost the same 2θ positions. According to the diffraction patterns, all films have a face-centered cubic (fcc) structure. It is seen that the peaks around 43° belong to the (111) plane of the fcc structure of Cu atoms. Also, it is determined that the peaks around 50° and 74° belong to the (200) and (220) planes of the fcc structure of Cu atoms. The obtained results are compatible with the JCPDS card numbered as 03–1018 for Cu atoms. Considering the high Cu content in the films, it is an explainable situation that the peaks formed by the reflections from Co atoms are invisible in the patterns. Increasing the number of bilayers and therefore the total film thickness did not cause a significant change in the peaks of the planes of the fcc structure. The crystallite size of the (111) plane was calculated by the Scherrer equation[25] and was found to be 10 nm for all films examined in this series. The results indicated that the examined multilayer structures had the same crystal structure. The strain values (ε) of the films were also calculated using the Williamson–Hall method[26] and the values were found to be 10.76×10^{-3}, 10.46×10^{-3}, 10.59×10^{-3} ($\pm$ 0.11) for total thicknesses of 120, 140, and 160 nm, respectively (see Table 1). It is seen that the ε values are almost stable for the different total thicknesses.

SEM images taken at 80k magnification of the surfaces of Co/Cu with total film thicknesses of 120, 140, and 160 nm are shown in Figure 3. When the SEM images are examined, it can be depicted that grainy structures are observed on the film surfaces and distribution of these grains on the film surface is almost homogeneous. According to scale bar in the SEM images, it can be considered that the diameter of the grains is around 25–35 nm and the increase in total thickness does not cause a significant change in the surface morphology. This is consistent with the atomic film contents determined by elemental analysis. Considering that all parameters, except the number of bilayers, are the same in the production of films with different thicknesses, it is expected that the atomic film composition, and therefore the surface morphology, are similar. On the other hand, a different thickness - morphology correlation from this study was reported in a previous study.[27] In study,[27] the effect of total thickness on the structural and magnetic properties of

Table 1. Results of structural and magnetic analysis for Co/Cu multilayers with different total thicknesses.

Total thickness (nm)	Co content (at. %)	Strain (ε) (± 0.11)	Rp (nm)	Ra (nm)	Rq (nm)	M_s (emu/cm^3)	H_c (Oe)	M_r (emu/cm^3)	M_r/M_S
120	11	10.76×10^{-3}	47	5.82	7.44	605	43	160	0.3
140	12	10.46×10^{-3}	63	6.74	8.77	605	52	393	0.7
160	15	10.59×10^{-3}	89	7.92	11.68	624	63	350	0.6

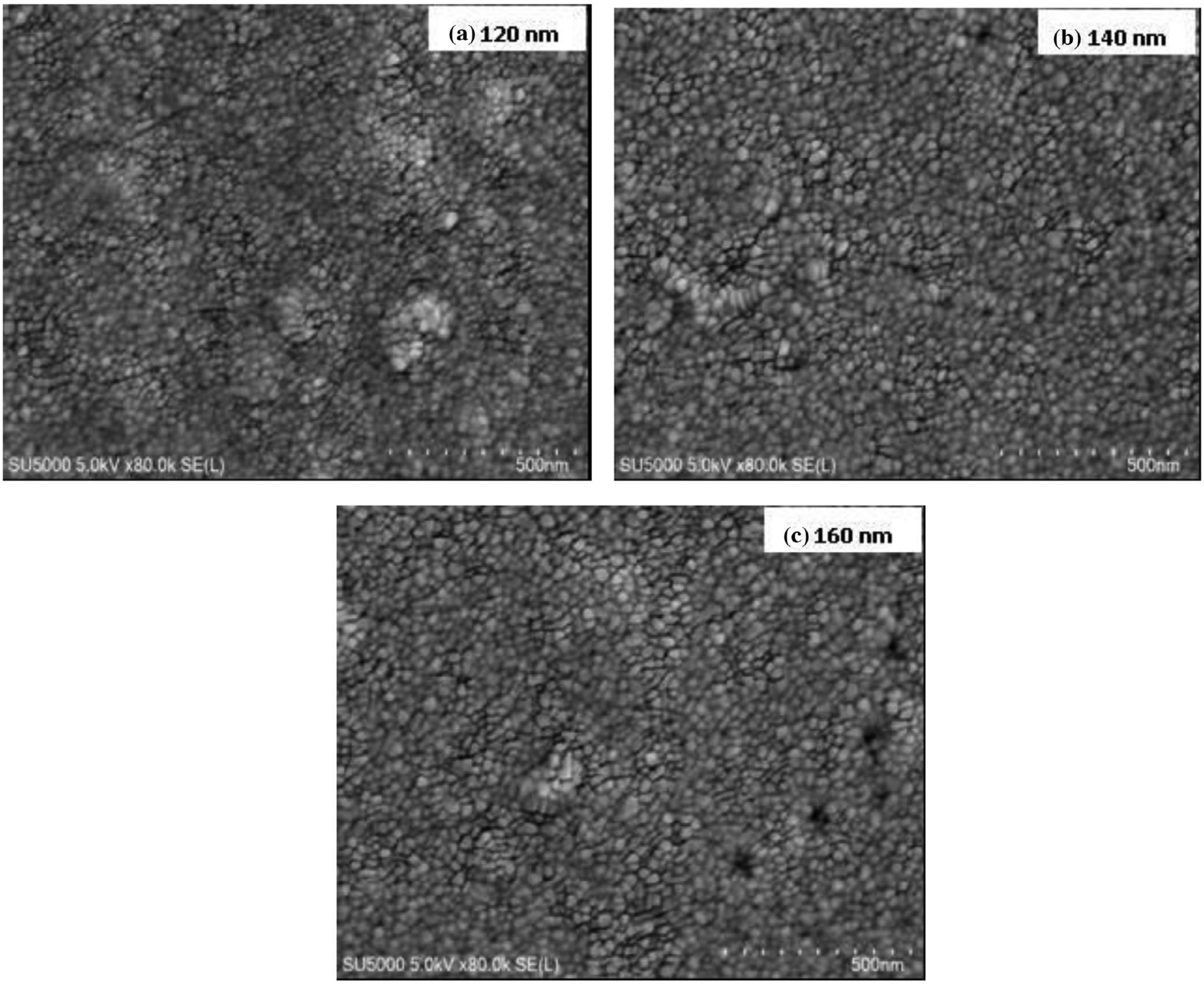

Figure 3. SEM images of Co/Cu multilayer films with different total film thicknesses: a) 120, b) 140, and c) 160 nm.

Ni/Cu films was investigated, and it was revealed that films with different thicknesses have different surface morphologies. The most important reason for the differences can be attributed to the difference in the magnetic component in the investigated material.

The AFM images of the Co/Cu films and those of the substrate surfaces are shown in Figure 4. According to the substrate image shown in Figure 4a, the substrates were determined to be suitable structures for film deposition on them in terms of surface roughness. In addition, the surface images of the films were completely different from that of the substrate (Figure 4). In Figure 4b–d, 3D surface images of Co/Cu films with total thicknesses of (b) 120, (c) 140, and (d) 160 nm are shown. There are some heights of different sizes on the surface of the film with a thickness of 120 nm. These heights are indicated by relatively lighter colors in the AFM image. The maximum value of the heights (Rp) was 47 nm, and the average roughness (Ra) and root mean square (Rq) values were 5.82 nm and 7.44 nm, respectively. When the film thickness is 140 nm, the height of the light-colored regions in the AFM image increases slightly, and the Rp, Ra,

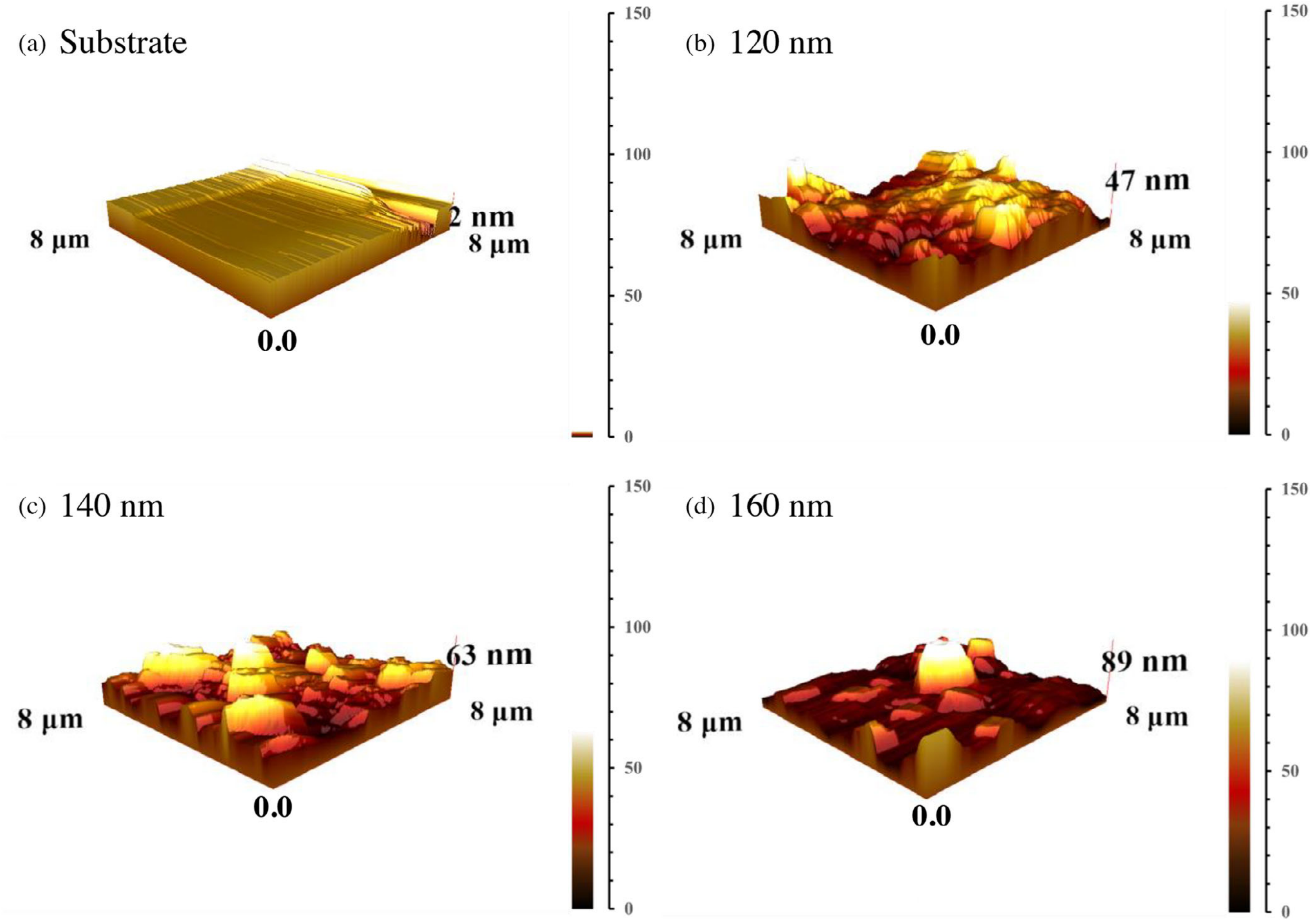

Figure 4. Three-dimensional AFM images (with altitude scale) of the substrate surface (a) and the surfaces of films with total thicknesses of 120 (b), 140 (c), and 160 nm (d).

and *R*q values are recorded as 63, 6.74, and 8.77 nm, respectively. Furthermore, the heights and roughness are more evident and larger as understood from both the light and dark-colored regions in the AFM figure of the film with 160 nm thickness. For the thickest film, the *R*p, *R*a, and *R*q values were found as 89, 7.92, and 11.68 nm, respectively. These values of the surface parameters (*R*p,a,q) are listed in Table 1. Consequently, a regular increase in the film thickness caused the surface roughness to increase gradually.

To investigate the effect of different total film thicknesses on the magnetic properties of the Co/Cu films, parallel hysteresis curves were obtained, and these curves are shown in Figure 5. From the curves, M_s, H_c, M_r, and M_r/M_s values were determined, and these values are presented in Table 1. The changes in the M_S and H_C values with respect to the total film thickness are shown in Figure 6. The M_s values were calculated according to the number of magnetic moments that reached magnetic saturation per unit volume. The M_s values obtained by gradually increasing the total film thickness to 120, 140, and 160 nm were 605 emu/cm^3, 605 emu/cm^3, and 624 emu/cm^3, respectively. Increasing the total film thickness resulted in the M_s values remaining approximately the same. This may be due to the slight change in the content of Co atoms, which is the ferromagnetic component in the film. Therefore, it is an expected result that M_s does not change considerably. It should be noted that the M_s values are mainly affected by the content ratios of the elements that form the magnetic material.[28]

For films with total thicknesses of 120, 140, and 160 nm, the H_c values were 43 Oe, 52 Oe, and 63 Oe, respectively. The gradual increase in H_c values with increasing total film thickness can be attributed to the increase in surface roughness. Our previous study[29] supports this relationship between surface roughness and H_c. Besides, Paul et al. reported in their study [7] that the number of bilayers affects the structural properties such as surface roughness and consequently the magnetic properties of multilayers. However, it was noted in[30] that H_c is generally affected by deposit thickness and reduced H_c values are achieved by considering relatively high thickness values, unlike the results obtained in the present study. The reason for this may be the different material types (multilayer, alloy, nanoparticle, etc.) or deposition technique. It was stated in study[30] that reverse pulse plating process in the electrodeposition technique was found beneficial in improving properties such as H_c in soft magnetic materials such as permalloys (Ni–Fe), even with increased film thickness. The study[30] also demonstrates the effect of the production technique on the magnetic properties.

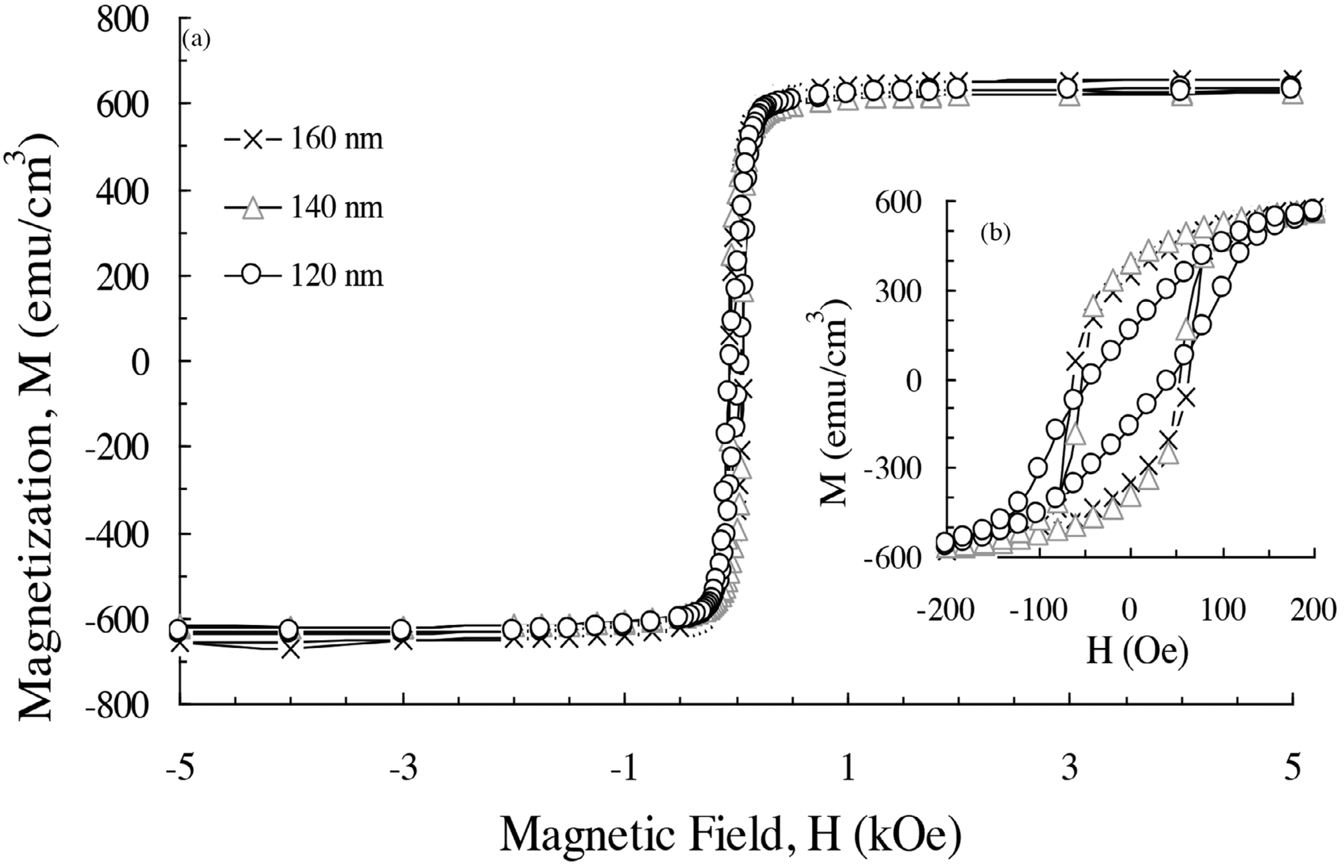

Figure 5. Hysteresis curves of Co/Cu films with different total thicknesses (the curves were plotted at magnetic field between a ± 5 kOe and b ± 200 Oe).

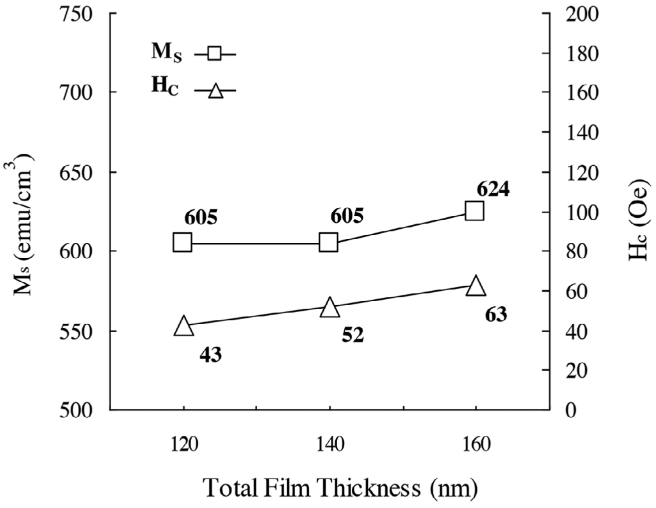

Figure 6. Change of M_s and H_c values for Co/Cu films with different total thicknesses.

However, when the H_c values are considered, it is realized that the films are generally closer to the properties of soft magnetic materials.[31] When the total thickness of Co/Cu magnetic films was 120, 140, and 160 nm, the M_r values were 160 emu/cm^3, 393 emu/cm^3, and 350 emu/cm^3, and the M_r/M_s values were 0.3, 0.7, and 0.6, respectively. According to results, it was determined that a general increase occurs in the M_r and M_r/M_s values as the film thickness increased.

2.1. Effect of Deposition Rate of Co Layer

Elemental analysis of the multilayers produced at different Co deposition rates was also executed using the EDX technique. When the deposition rate of the Co layer was 0.02 nm/s, the percentage of Co atoms in the thin film was 19%, and when the deposition rate was increased to 0.05 nm/s, the content of Co atoms increased to 22%. The content of Co atoms in the thin film was found to be 26% when the deposition rate of Co layer was gradually increased to 0.08 nm/s. It was also found that the remaining percentage of the film composition consisted of Cu atoms.

The XRD patterns of the Co/Cu thin films, in which the effect of different deposition rates of Co on the crystal structure was examined, are shown in Figure 7. The results of the crystal structure analysis of the substrate were given in the previously examined series. A main peak appeared at $2\theta = 43.6°$ when the deposition rate of the Co layer was 0.02 nm/s. Other peaks also appeared at $2\theta = 50.8°$ and $2\theta = 74.4°$ in the same pattern. In the XRD pattern of the second film which has deposition rate of 0.05 nm/s, there is a main peak at 2θ position of 43.6° and a distinct peak at 50.8° as similar to that of the pattern of the film deposited with the lowest Co deposition rate.

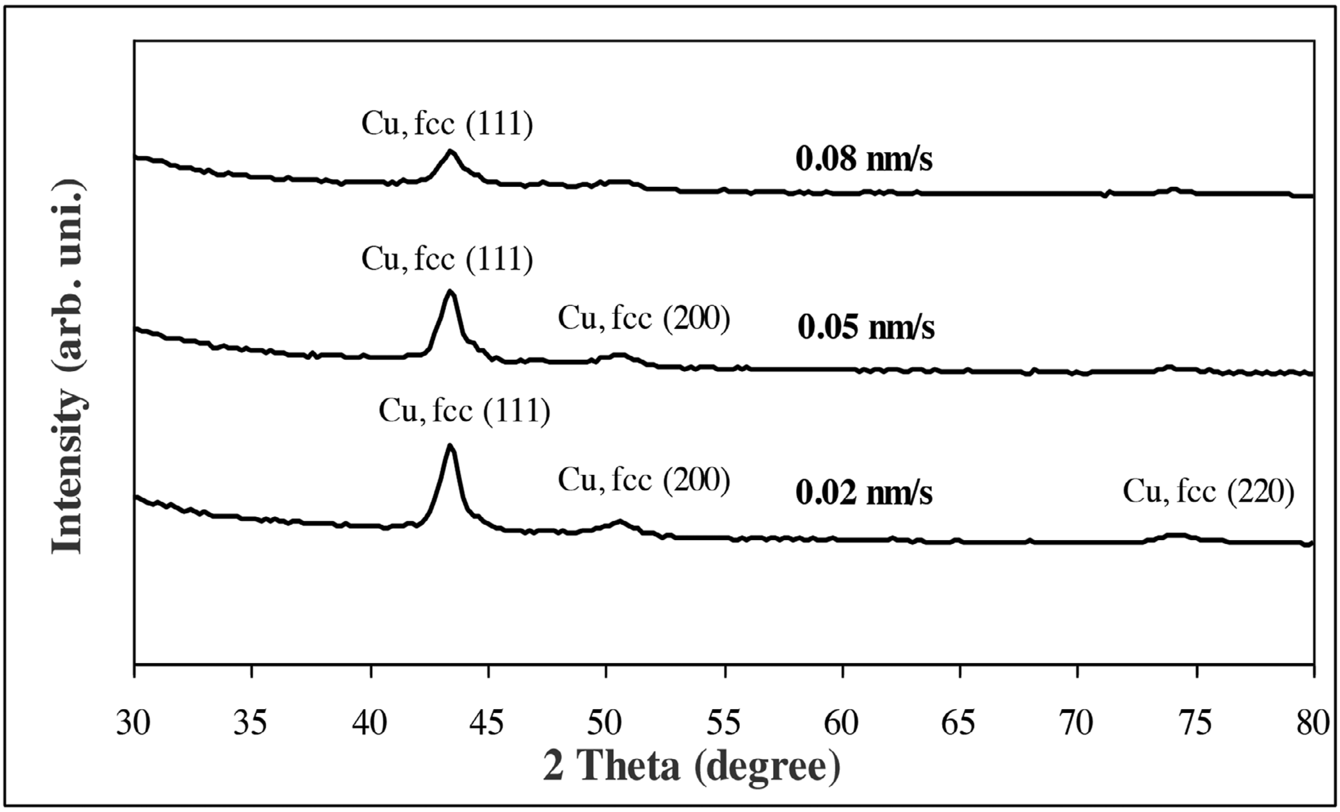

Figure 7. XRD patterns of Co/Cu films deposited with different deposition rates of the Co layer.

In the pattern of the film with a deposition rate of 0.08 nm/s, only a peak at $2\theta = 43.6°$ was observed (see Figure 7). According to the results, it was understood that the peak formed at $2\theta = 43.6°$ for all films was a peak belonging to the (111) plane of the fcc structure of Cu atoms. The intensity of this peak gradually decreased as the deposition rate increased systematically. In the diffraction pattern of the films with deposition rates of 0.02 nm/s and 0.05 nm/s, it was determined that the peaks appearing at $2\theta = 50.8°$ belonged to the characteristic (200) plane of the fcc structure of Cu atoms. For the lowest rate, the peak formed at 74.4° was labeled as (220) of the fcc structure of Cu atoms. However, this peak disappeared in the films with Co deposition rates of 0.05 nm/s and 0.08 nm/s at the same angle position. In other words, it was determined that the certain peaks belonging to the fcc structure of Cu atoms did not occur as the deposition rate of the Co layer increased. As a result, as the deposition rate increased, the Cu content decreased and the film turned into a single-crystal structure. The change in the deposition rate of the Co layer affected the crystal structure. The obtained results were compatible with the JCPDS card for Cu (03–1018). For deposition rates of 0.02 nm/s, 0.05 nm/s and 0.08 nm/s, the crystallite sizes of the (111) plane of the fcc structure were calculated as 10, 10, and 9 nm, respectively. Considering the change in film content, a decrease in this rate is notable. The decrease in the crystallite size of the fcc (111) plane with the increase in the content of the ferromagnetic material was found to be consistent with a previous study[32] in which the effect of the Ni layer thickness of Ni/Al films was investigated. The strain (ε) values of the films were calculated as 10.73×10^{-3}, 10.92×10^{-3}, and 12.12×10^{-3} ($\pm$ 0.11) for deposition rates of 0.02, 0.05, and 0.08 nm/s, respectively. The values are listed in Table 2. It is clearly seen that the strain in the structure increased with increasing Co deposition rate, especially for the highest deposition rate.

The SEM images obtained from the surface morphological analysis considering different deposition rates of the Co layer are shown in Figure 8. The SEM image for the deposition rate of 0.02 nm/s is shown in Figure 8a. Spherical granular grains were observed in this image. Figure 8b,c are the SEM images of the surfaces of the films with deposition rates of 0.05 nm/s and 0.08 nm/s, respectively. As can be seen in these figures, the surface structure observed for the lowest deposition rate continued to exist, but a slight decrease in the diameter of the grain size occurred. In particular, considering the films produced at high deposition rates, the surface morphologies shown in this study and[33] are similar. Consequently, the change detected in the SEM image may be related to the change in the peak intensities observed in the XRD pattern with the decrease in the percentage of Cu atoms in the content of the films.

The surface images of Co/Cu thin films obtained by AFM for deposition rates of (a) 0.02, (b) 0.05, and (c) 0.08 nm/s are shown in Figure 9. When Figure 9a is examined, some elevations of different sizes are noticeable on the surface of the film sputtered at a deposition rate of 0.02 nm/s. For the lowest rate, the Rp, Ra, and *R*q values were found as 132 nm, 17.17 nm, and 22.13 nm, respectively. There was a considerable decrease in these values, and the decrease continued as the deposition

Table 2. Results of structural and magnetic analysis for Co/Cu multilayers deposited with different deposition rates of Co layers.

Co deposition rate (nm/s)	Co content (at. %)	Strain (ε) ($\pm$ 0.11)	*R*p (nm)	*R*a (nm)	*R*q (nm)	M_s (emu/cm^3)	H_c (Oe)	M_r (emu/cm^3)	M_r/M_S
0.02	19	10.73×10^{-3}	132	17.17	22.13	824	46	388	0.5
0.05	22	10.92×10^{-3}	69	6.48	9.52	1029	43	638	0.6
0.08	26	12.12×10^{-3}	56	6.36	8.22	1072	36	507	0.5

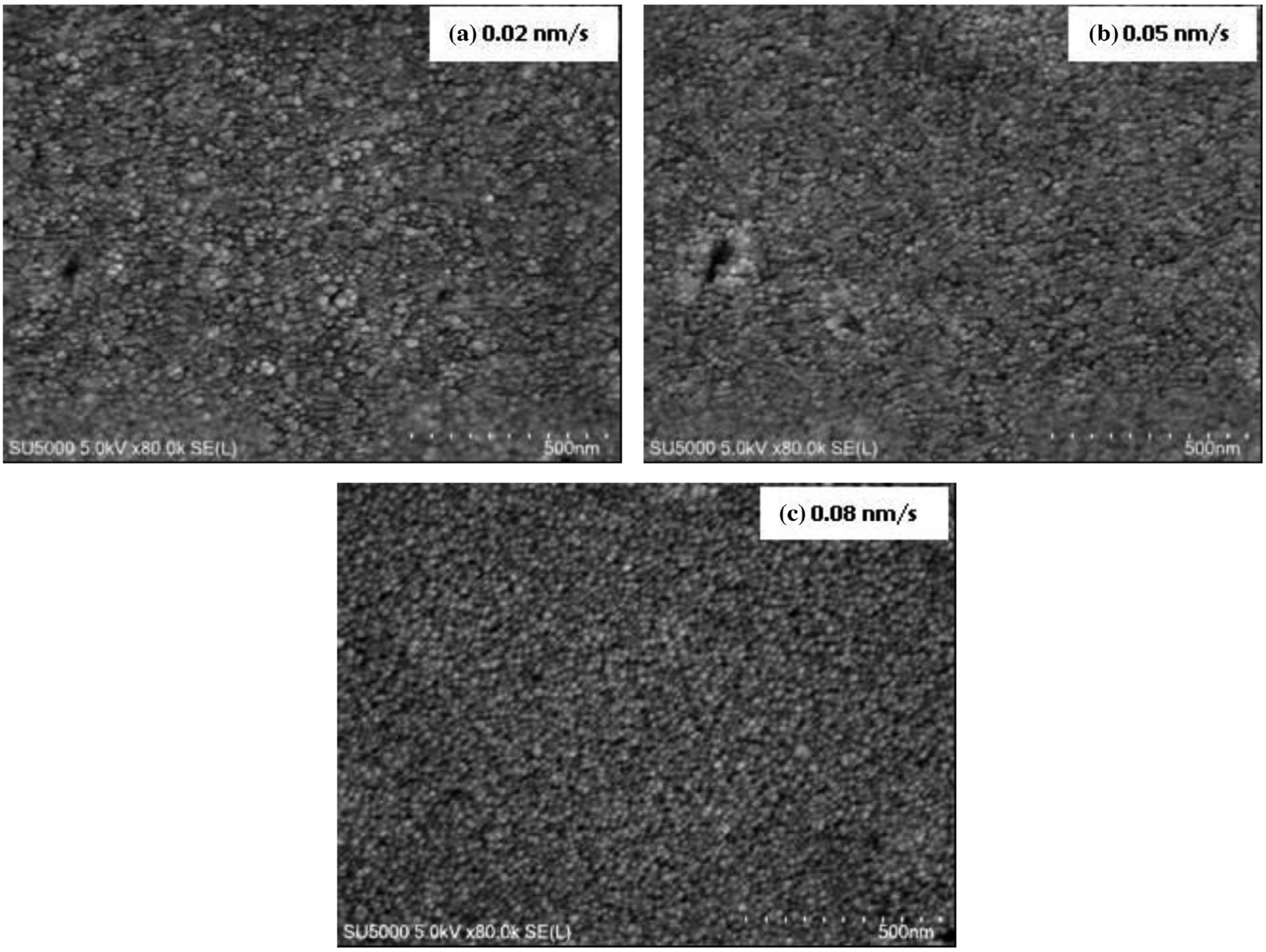

Figure 8. SEM images of Co/Cu films produced with different deposition rates of the Co layers: a) 0.02, b) 0.05, and c) 0.08 nm/s.

rate increased, as shown in Figure 9b,c, which represent the surfaces of two different films with deposition rates of 0.05 and 0.08 nm/s, respectively. The *R*p, *R*a, and *R*q values were 69, 6.48, and 9.52 nm, respectively, for the film deposited at a rate of 0.05 nm/s, and 56, 6.36, and 8.22 nm, respectively, for the highest deposition rate. The values of the surface parameters were also listed in Table 2 for the films sputtered at different deposition rates. As the deposition rate increased, the film surface became relatively smoother and less rough. In a previous study,[29] it was emphasized that different deposition rates affect the film surface, and smoother film surfaces can be obtained when relatively high deposition rates are applied. It can be concluded that the surfaces of the Co/Cu films produced at relatively high deposition rates are smoother and hence have a more suitable structure, which means less pinning effect on the magnetic domains, less hysteresis loss for relevant magnetic applications, and less surface stress.

To investigate the effect of different deposition rates of the Co layer on the magnetic properties, parallel hysteresis curves were obtained and shown in Figure 10. When the deposition rate of the Co layer was gradually increased from 0.02 to 0.05 nm/s and 0.08 nm/s, the M_s values also increased from 824 to 1029 emu/cm^3 and 1072 emu/cm^3, respectively. In other words, the increase in the deposition rate caused an increase in the atomic Co content, and thus a considerable increase in M_s values. As the Co content increased, the magnetization of the material also

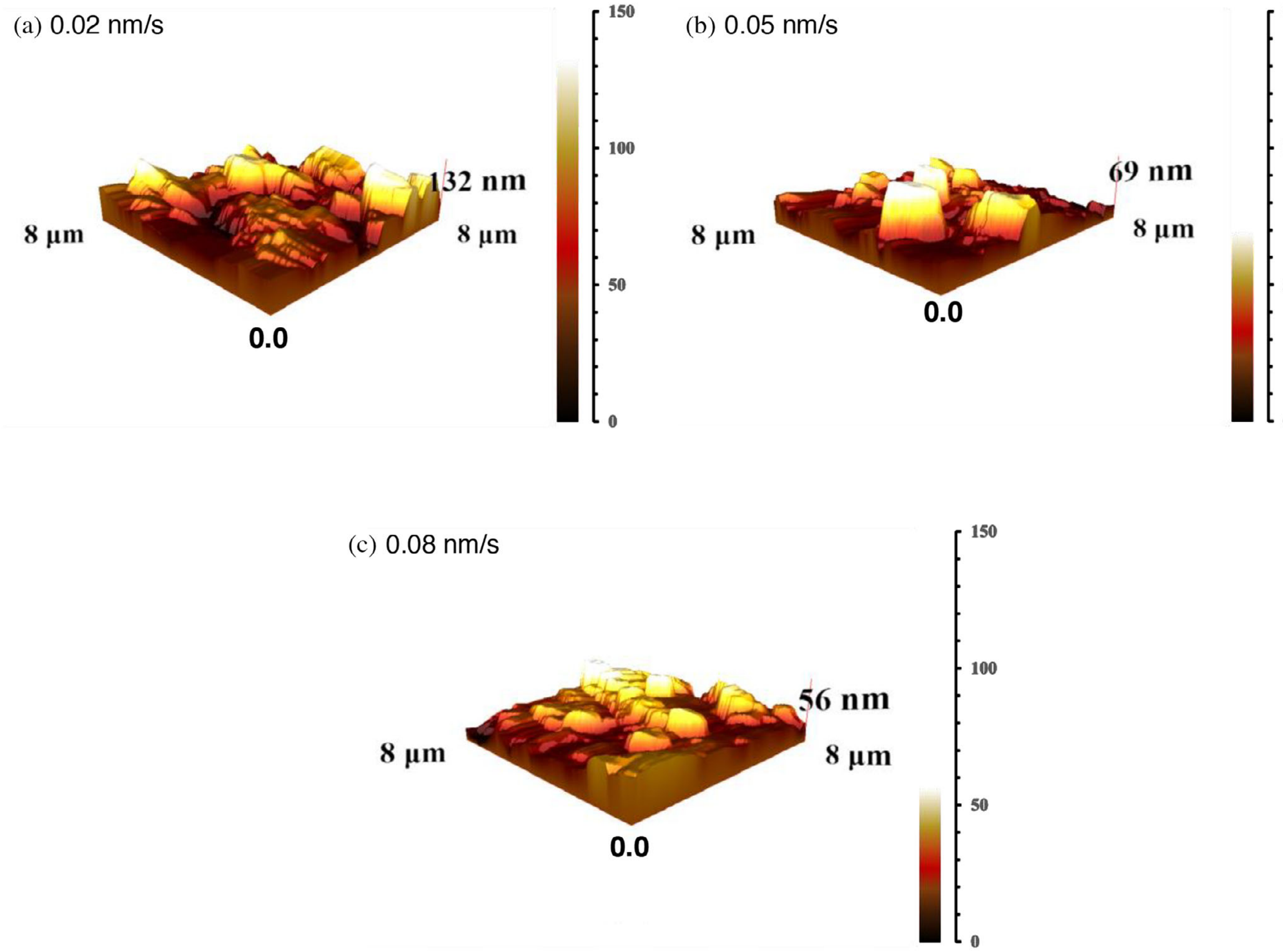

Figure 9. Three-dimensional AFM images (with altitude scale) of Co/Cu films sputtered at different deposition rates of Co layers, a) 0.02, b) 0.05, and c) 0.08 nm/s.

increased. In addition, the H_c values obtained for the films produced at Co deposition rates of 0.02, 0.05, and 0.08 nm/s are 46 Oe, 43 Oe, and 36 Oe, respectively. Accordingly, the increase in the deposition rate caused a gradual decrease in H_c values. It has been stated that an increase in the amount of nonmagnetic components in a magnetic material causes an increase in the H_c value of that material.[31,34] The main reason for the increase in the H_c is the enhancing effect of the grain boundary pinning in the magnetic material with the addition of nonmagnetic material, as explained in detail in.[34] Therefore, as the deposition rate of the produced thin films increased, the decrease in the Cu atom content may have caused the H_c values to decrease. On the other hand, the decrease in the crystallite dimensions of the (111) plane of the fcc structure may have contributed to this decrease in H_c values. A graph showing the change in M_s and H_c values with the Co deposition rate is presented in Figure 11. It has been clearly stated in the studies[32] and[35] that the surface morphology has significant effects on the H_c values of the films. It can be concluded that the change in surface roughness, which is also associated with the contraction of grain structures in the SEM images, contributes to the change in H_c values. Moreover, Anuniwat et al.[36] stated that the large increase in coercivity was attributed to the relaxation of film stress. In this case, the increase in the ε value at high deposition rates can be expected to lead to a decrease in the H_c values of the films. The increase in strain with increasing deposition rate may have suppressed the effects of defects and contributed the decrease in the H_C value. For deposition rates of 0.02, 0.05, and 0.08 nm/s, the M_r values of the films were found to be 388, 638, and 507 emu/cm^3, and the M_r/M_s ratios were determined as 0.5, 0.6, and 0.5, respectively. The analysis results obtained in this part are given in Table 2.

3. Conclusion

In the first series where the effect of total film thickness was examined, the atomic Co and Cu contents remained almost the same as the total thickness of the films increased. It was also observed that the films crystallized in the fcc structure of Cu atoms and the most intense peak for all total thicknesses belonged to the (111) plane. The XRD results were consistent with the atomic content. In addition, when the film thickness gradually increased from 120 to 160 nm, the surface roughness

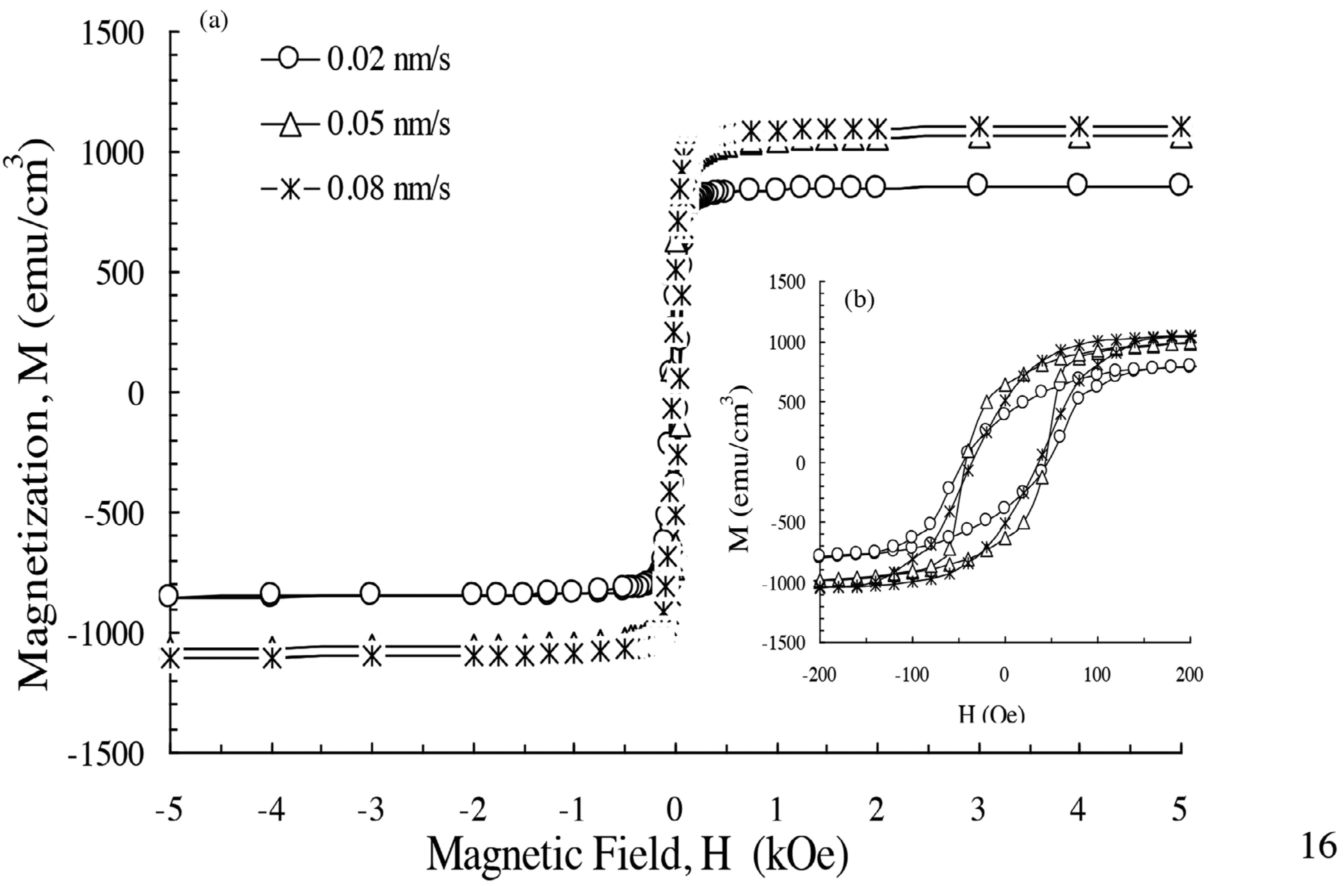

Figure 10. Hysteresis curves of Co/Cu multilayers deposited with different deposition rates of Co layer. Plotted between a) ± 5 kOe and b) ± 200 Oe.

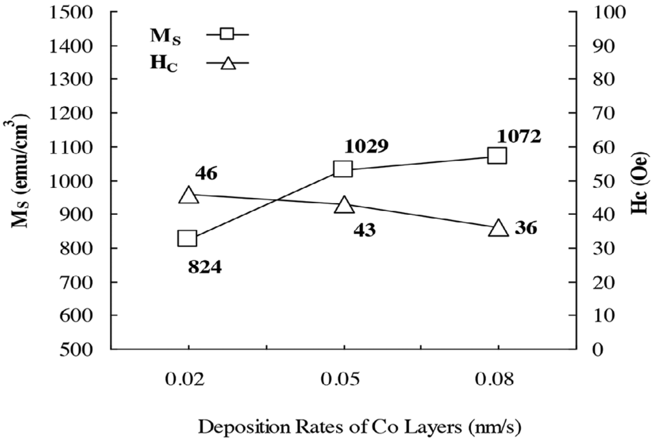

Figure 11. Changes in M_s and H_c values of Co/Cu films produced with different deposition rates of the Co layers.

increased, and therefore, a gradual increase in H_c values was detected, and the M_r/M_s value was approximately doubled. The change in the total film thickness had a significant effect on the H_c values, particularly because of the change in the surface properties. Regarding the effect of the Co deposition rate, the percentage of Co atoms increased as the deposition rate of the Co layer increased. The analysis indicates that all peaks correspond to Cu atoms. With the increase in the deposition rate of the Co layer, the peak intensity of the (111) plane of the fcc structure in the XRD pattern decreased, and the peaks of the (200) and (220) planes disappeared. Thus, the crystal structure was affected by the Co deposition rate. On the surfaces of film grown at high deposition rates, the size of the granular structures is relatively smaller. Considering the relatively high deposition rates, the roughness decreased and smoother surfaces were formed. The increase in strain and decrease in surface roughness, and therefore decrease in the effect of surface stress and defects, may have caused the H_c values to decrease. The increase in the deposition rate of the magnetic material affected the magnetic properties due to the change in the microstructural properties. This situation allows the desired magnetic properties to be obtained in applications where Co/Cu multilayer films are used.

Acknowledgments

The authors would like to thank Prof. Dr. Öznur KARAAĞAÇ for her contributions in achieving the VSM measurements. The authors would also like to thank Karamanoğlu Mehmetbey University, Scientific and Technological Research Application and Research Center (KMÜ BİLTEM) for the XRD and EDX analyses of the films, as well as the SEM and AFM images. This study was financially supported by the State Planning Organization/Turkey under grant no. 2005K120170 for Sputtering and VSM systems.

Conflict of Interests

The authors declare no conflict of interest.

Data Availability Statement

The data that support the findings of this study are available from the corresponding author upon reasonable request.

Keywords: Co/Cu multilayers · Deposition rates · Film thickness · Magnetic properties · Sputtered films

[1] A. Ghobadpoor, M. M. Eskandari, A. Zare, M. Karami, *Iran. J. Catal.* **2021**, *11*, 69–75.

[2] C. Gianfagna, H. Yu, M. Swaminathan, R. Pulugurtha, R. Tummala, G. Antonini, *J. Electron. Mater.* **2017**, *46*, 4963–4975, https://doi.org/10.1007/s11664-017-5487-8.

[3] P. Vavassori, E. Angeli, D. Bisero, F. Spizzo, F. Ronconi, *Phys. stat. sol.* **2002**, *189*, 423–427.

[4] J. R. Childress, R. E. Fontana Jr, *C. R. Physique* **2002**, *6*, 997–1012, https://doi.org/10.1016/j.crhy.2005.11.001.

[5] S. B. Darling, S. D. Bader, *J. Mater. Chem.* **2005**, *15*, 4189, https://doi.org/10.1039/b506357d.

[6] K. J. Kirk, *Contemporary Physics*, **2000**, *41*, 61-78.

[7] A. Paul, T. Damm, D. E. Bürgler, S. Stein, H. Kohlstedt, P. Grünberg, *J. Phys.: Condens. Matter* **2003**, *15*, 2471–2491.

[8] A. Tekgül, H. Köçkar, H. Kuru, M. Alper, *Z. Naturforsch., A:* **2018**, *73*, 127–133.

[9] [9] N. Ahmed, M. A. Iqbal, Z. S. Khan, A. A. Qayyum, *J. Electron. Mater.* **2020**, *49*, 4221–4230, https://doi.org/10.1007/s11664-020-08138-2.

[10] Y. Sik Jung, D. W. Lee, D. Y. Jeon, *Appl. Surf. Sci.* **2004**, *221*, 136–142, https://doi.org/10.1016/S0169-4332(03)00862-6.

[11] C. Boeglin, O. Ersen, M. Pilard, V. Speisser, F. Kronast, *Phys. Rev. B* **2009**, *80*, 035409, https://doi.org/10.1103/PhysRevB.80.035409.

[12] N. Rajasekaran, J. Mâni, B. G. Toth, G. Molnâr, S. Mohan, L. Peter, I. Bakonyi, *J. Electrochem. Soc.* **2015**, *162*, D204–D212, https://doi.org/10.1149/2.0451506jes.

[13] K. Liu, R. Zhang, L. Lu, J. Li, S. Zhang, *Coatings* **2023**, *13*, 2097, https://doi.org/10.3390/coatings13122097.

[14] G. R. Pattanaik, D. K. Pandya, S. C. Kashyap, *Thin Solid Films* **2003**, *433*, 247–251, https://doi.org/10.1016/S0040-6090(03)00293-1.

[15] Q. Liu, J. H. Min, J. U. Cho, Y. K. Kim, *IEEE Trans. Magn.* **2005**, *41*, 930–932.

[16] O. A. Kondratev, I. A. Makhotkin, S. N. Yakunin, *Appl. Surf. Sci.* **2022**, *574*, 151573, https://doi.org/10.1016/j.apsusc.2021.151573.

[17] M. Tokaç, *Appl. Magn. Reson.* **2024**, *55*, 1389–1402.

[18] Y. Zhang, X. Li, Y. Zhang, J. Liu, B. Dai, Y. Ren, *Appl. Phys. A* **2024**, *130*, 96, https://doi.org/10.1007/s00339-023-07273-x.

[19] V. Dalouji, N. Rahimi, A. R. Souri, *Adv. Ceram. Prog.* **2022**, *8*, 29–38.

[20] R. Garg, S. Gonuguntla, S. Sk, M. S. Iqbal, A. O. Dada, U. Pal, M. Ahmadipour, *Adv. Colloid Interface Sci.* **2024**, *330*, 103203, https://doi.org/10.1016/j.cis.2024.103203.

[21] M. A. Salari, G. M. Muğlu, V. Şenay, S. Sarıtaş, M. Kundakçı, *Ceram. Int.* **2024**, *50*, 39221–39225, https://doi.org/10.1016/j.ceramint.2024.07.291.

[22] M. Ojha, A. A. Elmustafa, *J. Mater. Sci.: Mater. Electron.* **2024**, *35*, 1100.

[23] Y. Ma, X. Xie, H. Chen, T. Zhang, T. T. Debela, *Vacuum* **2021**, *194*, 110625, https://doi.org/10.1016/j.vacuum.2021.110625.

[24] V. Tiron, E. L. Ursu, D. Cristea, G. Bulai, G. Stoian, T. Matei, I. L. Velicu, *Nanomaterials* **2022**, *12*, 512, https://doi.org/10.3390/nano12030512.

[25] M. S. Hossain, S. Ahmed, *Results Mater.* **2023**, *20*, 100492, https://doi.org/10.1016/j.rinma.2023.100492.

[26] G. K. Williamson, W. H. Hall, *Acta Metall.* **1953**, *1*, 22–31.

[27] S. Çölmekçi, A. Karpuz, H. Köçkar, *J. Magn. Magn. Mater.* **2019**, *478*, 48–54.

[28] D. Flynn, M. P. Y. Desmulliez, *IEEE Trans. Magn.* **2010**, *46*, 979–985, https://doi.org/10.1109/TMAG.2009.2036723.

[29] A. Karpuz, H. Köçkar, S. Çölmekçi, M. Uçkun, *J. Supercond. Novel Magn.* **2020**, *33*, 463–472, https://doi.org/10.1007/s10948-019-05207-4.

[30] F. Zoia, R. Cesaro, R. Bernasconi, L. Magagnin, *Transactions of the IMF* **2025**, *103*, 12–20, https://doi.org/10.1080/00202967.2024.2435123.

[31] D. Jiles, *Introduction to Magnetism And Magnetic Materials*, Chapman and Hall Press, London **1991**, https://doi.org/10.1007/978-1-4615-3868-4.

[32] A. Karpuz, H. Köçkar, S. Çölmekçi, *Acta Phys. Pol. A* **2018**, *134*, 1180–1186, https://doi.org/10.12693/APhysPolA.134.1180.

[33] N. Kaplan, A. Karpuz, H. Köçkar, *Phys. Scr.* **2024**, *99*, 065975, https://doi.org/10.1088/1402-4896/ad48c7.

[34] G. P. Zhao, L. Zhao, L. C. Shen, J. Zou, L. Qiu, *Phys. B* **2019**, *28*, 077505.

[35] H. Köçkar, N. Kaplan, A. Karpuz, H. Kuru, B. Kaya, *J. Supercond. Novel Magn.* **2019**, *32*, 2457–2465.

[36] N. Anuniwat, M. Ding, S. J. Poon, S. A. Wolf, J. Lu, *J. Appl. Phys.* **2013**, *113*, 043905, https://doi.org/10.1063/1.4788807.

Manuscript received: August 28, 2025